Melting of systems of hard disks by Monte Carlo simulations

Julio F. Fernández,[1,*] Juan J. Alonso,[2] and Jolanta Stankiewicz[1]
[1]*Instituto de Ciencia de Materiales de Aragón, Consejo Superior de Investigaciones Científicas and Universidad de Zaragoza, 50009 Zaragoza, Spain*
[2]*Laboratoire de Physique et Mécanique des Milieux Hétérogènes, Ecole Supérieure de Physique et Chimie Industrielles, 10 rue Vauquelin, 75231 Paris Cedex 05, France*
(Received 7 June 1996; revised manuscript received 18 September 1996)

Monte Carlo (MC) results are reported for the melting of two-dimensional systems of N hard disks in the NpT ensemble both for hard crystalline walls (for $N=900$, 3844, and 15 876), and for periodic boundary conditions (for $N=64$, 256, 400, 576, 1024, and 4096). Long Monte Carlo runs (e.g., up to 35×10^6 MC sweeps for $N=15\,876$, and 2×10^8 MC sweeps for $N=1024$) give *equilibrium* results. We obtain mean values and fluctuations of the volume, of the orientational order parameter ϕ, and of the crystalline structure factor. Our main conclusions follow: (1) the melting transition is of second order; (2) $\langle\phi\rangle$ drops discontinuously (from $\langle\phi\rangle=0.74\pm0.02$) to zero at the melting point; and (3) we find no hexatic phase (if it exists for systems of hard disks, then the range for it is within about 1% of the melting volume value). [S1063-651X(97)10201-X]

PACS number(s): 64.70.Dv, 61.20.Ja, 05.70.Fh

I. INTRODUCTION

Despite the enormous effort spent studying two-dimensional melting over a time span of several decades, the nature of this phase transition remains a matter of controversy. It differs qualitatively from melting in *three* dimensions. As was first shown by Peierls [1] and by Landau [2], long wavelength phonons destroy long-range crystalline order in two dimensions (that is, the density cannot be a periodic function of position over all space). A rigorous proof of it was provided by Mermin, who also pointed out that orientational long-range order can nevertheless exist in two dimensions (2D) [3]. The theory of Nelson and Halperin (NH) was an important step toward understanding melting in 2D [4,5]. In this theory, free dislocations destroy weak crystalline order above the melting point, much as free vortices destroy weak magnetic long-range order in the paramagnetic phase of the XY model in 2D, in the theory of Kosterlitz and Thouless [6]. However, since dislocations do not, by themselves, obliterate orientational order, the existence of a noncrystalline, nonisotropic phase (referred to by NH as the *hexatic* phase) is, therefore, possible in this theory. Other topological defects (referred to as *disclinations* by NH) would destroy orientational order completely when the system is expanded beyond a second critical point into the *isotropic* phase.

Let v_m and v_i be the specific volumes for the crystalline-hexatic and for the hexatic-isotropic transitions, respectively. The main predictions of NH are (1) density correlations decay algebraically with distance in the crystalline phase, with a critical index η that increases with v up to $\eta<\frac{1}{3}$ at $v=v_m$; (2) as v increases, the orientational order parameter drops discontinuously (by an undetermined amount) to a null value at $v=v_m$; (3) in the hexatic phase, density correlations decay exponentially, while orientational correlations decay algebraically with distance (with a critical index η_6 that varies between $\eta_6=0$ at $v=v_m$ and $\eta_6=\frac{1}{4}$ at $v=v_i$); and (4) the critical behavior of the orientational correlation length in the isotropic phase is given by $\xi_6\sim\exp(b/\sqrt{v-v_i})$. The extent of the hexatic phase was not determined by NH (v_i-v_m may in fact vanish altogether).

Other melting mechanisms, such as grain boundary formation [7] have also been proposed. Many experimental results [8–10] seem to support the two-stage melting scheme that has come to be known as the theory of Kosterlitz, Thouless, Halperin, Nelson, and Young (KTHNY) [4–6]. Many computer simulations had already been performed before the KTHNY theory came about [11,12]. Computer runs were necessarily short then, and no firm conclusions could be reached. Later, some support for the KTHNY scenario was drawn from some [13–15] but not all molecular dynamics simulations [16]. On the other hand, first order transitions have most often been diagnosed from Monte Carlo (MC) simulation results [17–22]. Lee and Strandburg recently obtained *equilibrium* results for small systems through MC simulations, in the constant pressure ensemble, of up to a few hundred disks for about 10^7 MC sweeps [20]. They obtained results for volume fluctuations and the free energy barrier, ΔG, between the solid and the liquid phases. Knowledge of volume fluctuations is important because the latent heat ΔQ of the transition, if there is one, follows from it ($\Delta Q=p\Delta V$ for a system of hard disks, since there is no internal energy). In addition, ΔG must increase as the system's surface for a first order transition [23]. Lee and Strandburg's data for systems of up to a few hundred particles show a trend that points to a first order phase transition. Our own results [24], and those of Bagchi, Andersen, and Swope [25], seem to be the only recent ones to come out of MC work that lend some support to the KTHNY theory. However, our results differ from those of Bagchi, Andersen, and Swope for the hexatic phase. Whereas we find no trace of it for a system of hard disks, they do, over an approximately

*Electronic address: jefe@posta.unizar.es

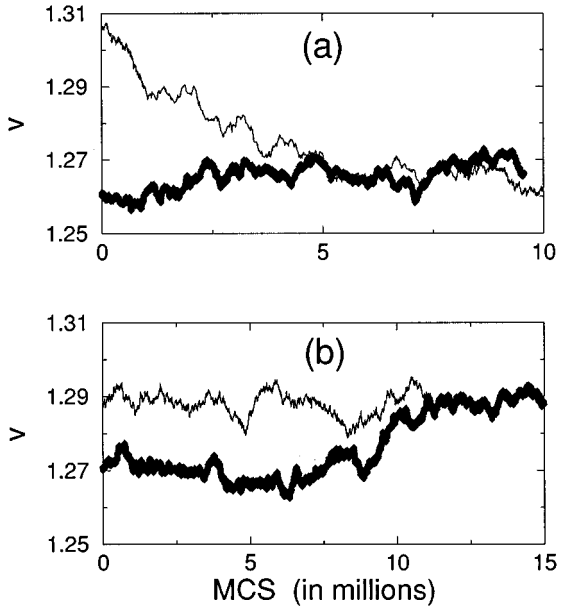

FIG. 1. (a) Volume vs MC sweeps for systems of 15 876 disks with hard crystalline walls, for $p=7.90$, for two different initial configurations: one obtained from previously expanding a dense ordered state, and the other one obtained from previously compressing a dilute disordered state. (b) Same as in (a) but for $p=7.875$.

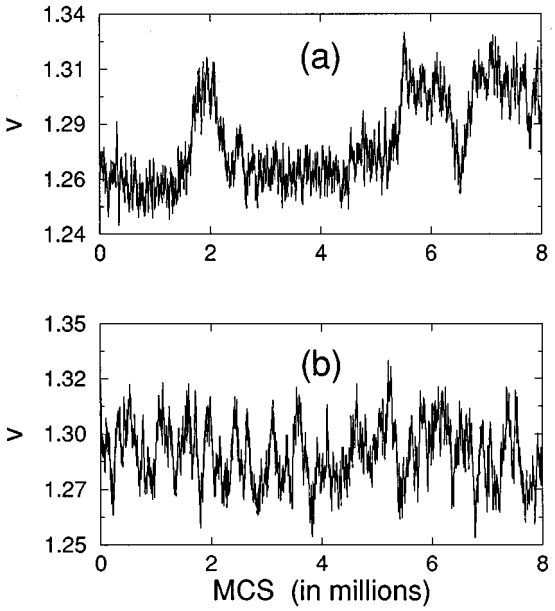

FIG. 2. (a) Chart of volume vs MC sweeps for a system of 1024 disks with PBC's not far from the critical point for $p=7.965$. It is a small part of a run of 3×10^8 MC sweeps. (b) Same as in (a) for a system of $N=900$ with HCW's for $p=7.77$, not far from the critical point. It is a large part of a run of 10^7 MC sweeps.

1% wide density range, for systems of particles interacting through $1/r^6$ potentials [26].

Monte Carlo simulations have suffered from finite size effects and limited computer running times. These two effects are not separable. As Zollweg and Chester pointed out, the equilibration time τ for systems of about 10^4 disks can be much longer than 10^6 MC sweeps [27]. This is illustrated in Fig. 1 for 15 876 disks. Very long simulations are needed because $\tau \propto L^z$ (where $z \simeq 2$ is expected), at the critical point (and, even worse, τ increases exponentially with L within a first order transition region). Thus, whereas Lee and Strandburg [20] found it sufficient to do 10^7 MC sweeps for systems of 256 particles, we did many runs of over 2×10^8 MC sweeps for systems of 1024 particles.

Equilibrium results for 2D systems of hard disks, obtained from MC simulations with both hard crystalline wall (HCW) and periodic boundary conditions (PBC's), are reported here. Our simulations are longer than any other ones previously reported by at least an order of magnitude. We have used the Metropolis algorithm in the constant pressure ensemble (that we shall hereafter abbreviate as the *NpT ensemble*) [12,18,20]. Some results for HCW boundary conditions have already been published [24]. Here we give additional results and further details. We have not published any of our results for PBC before. Because much of the work reported here had not been done at the time of publication of Ref. [24], some numerical results given in this paper may differ slightly from those therein.

A brief explanation for our choice of boundary conditions follows. The HCW boundary conditions (described in Sec. II) we use here have advantages over PBC's. Equilibration times are much shorter for systems with HCW's. This is because HCW's break the symmetry of the system. The importance of symmetry breaking in phase transition work was first emphasized by Bogolyubov [28]. We can obtain reliable equilibrium values for volume fluctuations $\langle(\delta v)^2\rangle$ for systems of many thousands of particles only because equilibration times are not as forbiddingly long for HCW's as they are for PBC's. This is illustrated in Fig. 2. The system of 900 disks with HCW's fluctuates well over an order of magnitude faster than the system of 1024 disks with PBC's. However, since all previous MC simulations for melting in 2D that we know of had used PBC's, the question naturally arises whether the difference between the conclusions we draw for HCW's and those of others [17–22] follow from the difference in boundary conditions. This question is important here, since the relevant correlation length exceeds the linear size of the system in regions of interest to us. In order to be able to compare readily our numerical results and conclusions with MC results that were obtained previously only for PBC's, we also report results we obtained for (smaller) systems with PBC's. We also obtain, as an unexpected bonus, results that are complementary to the ones obtained for systems with HCW's (e.g., probability distributions for the order parameter that yield interesting information that is unavailable for HCW's).

The plan of the paper is as follows. The boundary conditions, the algorithm used, the issue of equilibration times, and further details about our computer runs are discussed in Sec. II. In Sec. III, results for the pressure versus volume $p(v)$ and volume fluctuations $\langle(\delta v)^2\rangle$ are given. Data points for $\langle(\delta v)^2\rangle$ obtained both directly and from derivatives (taken numerically) of $p(v)$ are compared as a check on the goodness of the equilibrium averages obtained. $\langle(\delta v)^2\rangle$ is examined as a function of system size. The evidence runs counter to a first order phase transition. A volume discontinuity Δv for a first order phase transition, if evidence of it

were to turn up for larger values of N, would have to be less than 1% of the volume value upon melting. In addition, probability distributions for the volume, $P(v)$, are obtained from frequency of occurrence of v in MC runs. Values for the free energy barrier, ΔG, between the solid and the liquid phases follow from $P(v)$. Both $\langle(\delta v)^2\rangle$ and ΔG are examined as functions of system size. It is found that the trend reported by Lee and Strandburg [20] for smaller systems in favor of a first order phase transition is reversed for larger systems. This is further evidence against a first order phase transition. In fact, $P(v)$ for systems with hard crystalline walls with up to 3844 particles do *not* even show a double hump as a function of system volume (corresponding to $\Delta G=0$). According to the KTHNY theory of melting in two dimensions [4], there is a singularity in the bulk modulus, B, at the melting point. We obtain the melting volume value, $v_m=1.259\pm0.006$, from the locations of the maximum values of $|dB/dv|$. In Sec. IV, the average value, fluctuations and fourth-order cummulants of the orientational order parameter (ϕ, defined therein) are examined. Data for $\langle\phi\rangle$ show that $\langle\phi\rangle$ drops to zero discontinuously upon melting. Plots of $\langle(\delta\phi)^2\rangle$ versus $\langle\phi\rangle$, for systems of different sizes provide further evidence that $\langle\phi\rangle$ does not vanish continuously as $v\to v_m$ in the crystalline phase. Moreover, probability distributions $P(\phi)$ for ϕ exhibit a sort of coexistence between disordered states and $\phi=0.74\pm0.02$ states. [$P(\phi)$ is approximately size independent for $64\leqslant N\leqslant1024$, once again in accordance with a second order phase transition.] Yet further evidence that supports the conclusion that $\langle\phi\rangle$ vanishes discontinuously upon melting, as predicted by Nelson and Halperin, is provided in Sec. IV: a plot of $\langle(\delta|\phi|)^2\rangle$ versus $\langle\phi\rangle$, for systems of different sizes. Plots of fourth order cummulants of ϕ versus $\langle\phi\rangle$ are also consistent with a discontinuity in $\langle\phi\rangle$. Bounds for the extent (about a 1% volume change) of an intermediate phase (the *hexatic* phase), if one were to exist, also follows from the data shown in Sec. IV. Finally, some concluding remarks are made in Sec. V.

Throughout this paper the specific volume (actually an *area* in 2D) v is given in units of the closest packing volume, a_0, in the triangular lattice, and the pressure p is given in units of kT/a_0 throughout, where k is Boltzmann's constant and T is the temperature. All errors quoted for values of the average volume, for the order parameter and for its fluctuations, were computed as follows. After equilibration, each run was divided into five intervals; the standard deviation of the five corresponding values of the quantity of interest is given as its error.

II. ALGORITHM AND BOUNDARY CONDITIONS

A. Boundary conditions

We use both hard crystalline wall (HCW) and periodic boundary conditions. As HCW boundary conditions have not, as far as we know, been used before, a brief explanation for them follows. Consider a rectangular box of aspect ratio $\sqrt{3}\times2$ that produces no strains in a triangular crystal lattice. Let all ''sites'' on the boundary be occupied by disks, as in Fig. 3. They make up the ''crystalline'' walls. The positions (but not the sizes) of the disks that make up the HCW's

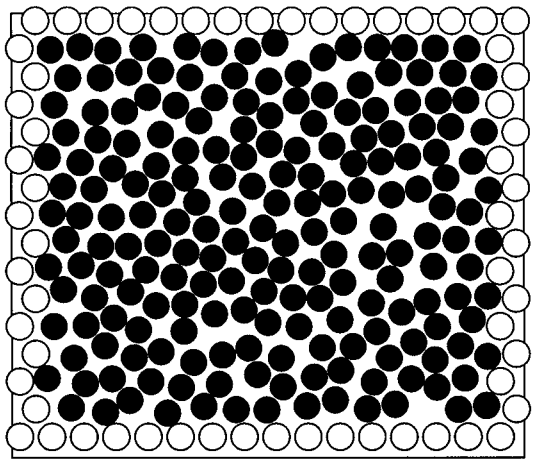

FIG. 3. Configuration of $(2^4-2)^2$ particles with hard crystalline walls. The white disks are fixed on triangular lattice sites. They make up the *crystalline* walls. The $N=(2^n-2)^2$ black disks ($n=4$ in this illustration) inside the walls are the system's particles. All disks, white and black, are always kept of equal size.

remain fixed throughout the simulation. $N=(2^n-2)^2$ disks inside the box are the system's ''particles.'' All 2^{2n} disks are of equal size, and remain so as their radii vary in unison (simulating volume variations of the system). For $v\gtrsim4a_0$, where a_0 is the closest packing volume, escape through gaps between fixed disks would be possible if there were no additional constraints, such as periodic boundary conditions (PBC's). For $v>4a_0$ these conditions may be thought of as PBC's plus a symmetry breaking array of fixed scatterers on the boundaries. Here $\langle v\rangle<1.5a_0$ and $\langle(v-\langle v\rangle)^2\rangle^{1/2}<0.014a_o$ (see below). Consequently, v never comes close to one-half of $4a_0$ in our simulations, and HCW's behaved therefore as impenetrable walls throughout. Because they break the symmetry of the system, HCW's ease nucleation of crystal growth, much as is done experimentally when crystals are grown from the melt *on a substrate*. Systems of 10^3 disks, for instance, turn out to equilibrate at least 10 times faster for HCW's than for PBC's.

B. Algorithm

We perform MC simulations for a hard disk system with a constant number of particles, pressure, and temperature; that is, in the so called NpT ensemble. In it, whether an attempted change of the system's particle configuration and/or volume is made or not, depends on the value of $\Delta\Omega/kT\equiv N\Delta\ln(V)+(\Delta E+p\Delta V)/kT$, where ΔE and ΔV are the corresponding changes in energy and volume, respectively. Detailed balance must, of course, be obeyed, so that if some transition is allowed with probability 1 when $\Delta\Omega<0$, then the corresponding reverse transition must take place with probability $\exp(-\Delta\Omega/kT)$. (See Refs. [12,18,20] for further details.) We implement it as follows: after all N particles in the system are given a chance to move, an attempt at changing the system volume is made. We do not allow particle moves beyond a distance of $\sqrt{a_o}/8$, which gives an acceptance rate of about a 40%. We then attempt to increase or decrease all particle radii (including the ones that make up the walls) by the same amount with equal probabil-

ity. Particle radii are increased only if no overlap ensues between any two disks. Attempts to make all disk radii smaller (corresponding to a total volume *increment* of ΔV) are only realized a fraction of the times given by $\exp[-\Delta\Omega/kT]$ (with $\Delta E=0$, since smaller radii produce no disk overlaps). That simulates variations of the system's volume. Specific volume variations larger than $\Delta v=2/Np$ are not allowed. Much larger variations would inconveniently reduce the acceptance rate.

In order to save time in the search for any overlap between pairs of disks that might arise whenever a disk is moved, we use a cell method that is described next. The choice of cell size is guided by the following considerations. We want cells that are too small to be able to lodge two disks in them. On the other hand, fewer neighboring cells have to be inspected for possible overlaps between pairs of disks for large cell sizes. Taking into account the range of particle densities of interest to us, we divide the system's box into $4^n\times 4^n$ rectangular cells. (Only one out of four cells are occupied.) A table that is updated whenever a particle moves lets us know which particle is in any given cell at all times. In order to save computer time, we let particle coordinates be integers that can be as large as 2^{30}. This enables us to assign cells to particles, after they move, with one single logical programming instruction.

C. Running times

As is remarked above, very long MC simulations are needed in order to obtain good *equilibrium* results. Volume fluctuations are specially slow. That is because the acceptance rate becomes very small if $\Delta v \gg kT/pN$, since, $\exp(-pN|\Delta v|/kT)\ll 1$ then, and $|\Delta v|\gg 1/pN$ would lead to some pairs of disks overlapping with a high probability for $\Delta v<0$.

1. Hard crystalline walls

The evolution of the volume of a system of 15 876 disks is shown in Fig. 1(a) for two different initial conditions: a disordered configuration and an ordered one. The disordered configuration was obtained by previously compressing the system from another disordered configuration at lower density. The ordered configuration was obtained by previously expanding the system from another completely ordered configuration at a higher density. Both evolutions in Fig. 1(a) are for $p=7.90$. Similarly, in Fig. 1(b), for $p=7.875$. It takes the system nearly 10^7 MC sweeps to equilibrate. Data points for the largest systems we have examined were obtained from *pairs* of runs —one of them coming from a disordered state and the other one originating from a crystalline configuration. Averages were performed only after convergence had been achieved. ''Maps'' for local bond orientation (to be explained below), as well as crystalline structure factor graphs, are shown in Figs. 13 and 14, respectively, for all four final states of the runs shown in Fig. 1. There is no apparent history dependence.

Our runs vary in length with N and with p. In addition to many shorter runs, at least seven runs were performed in the $(40–100)\times 10^6$ MC sweeps range for $N=$ 900, five runs in the $(20-50)\times 10^6$ MC sweeps range for $N=$ 3844, and eight runs in the $(10–35)\times 10^6$ MC sweeps range for $N=$ 15 876.

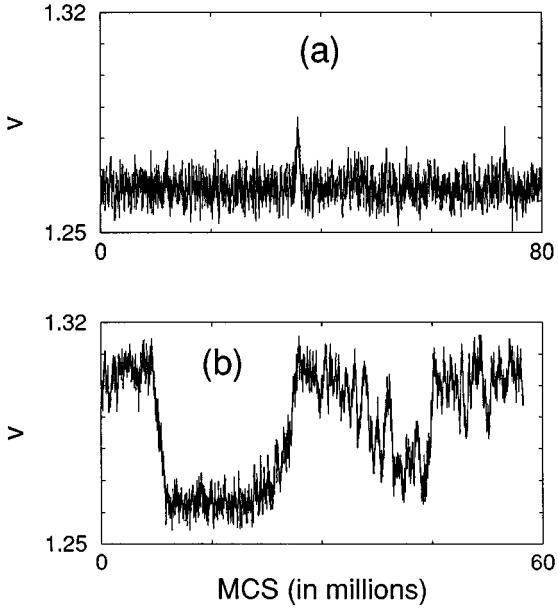

FIG. 4. (a) Specific volume vs MC sweeps for a system of 4096 disks, with PBC's, for $p=7.9175$. (b) The same as in (a), but at a slightly higher pressure $p=7.92$. The fact that v is larger in (b) than in (a) shows that equilibrium is not achieved in these runs.

2. Periodic boundary conditions

We estimate the time scale necessary to obtain equilibration and reliable equilibrium averages for PBC's from time evolutions such as the one shown in Fig. 2(a). Relaxation ''times'' for systems of 1024 particles can be as long as about 10^7 MC sweeps. [For a comparison with time scales for systems of about equal size but with hard cristalline walls, see Fig. 2(b).]

Figure 4 shows charts of volume versus ''time'' for a system of 4096 particles. The longest evolution [shown in Fig. 4(a)] is for $p=7.9175$. It might be thought that the system is in equilibrium. The other evolution, the one that shows large volume fluctuations [shown in Fig. 4(b)], is for a slightly *larger* pressure, $p=7.92$, which should yield a smaller mean value of the volume *in equilibrium.* Since it does not, it follows that equilibration has not in fact been achieved. Thus for systems of 4096 particles with PBC's, nearly 10^8 MC sweeps seem insufficient for equilibration to ensue in the critical region. For this reason, we give results for systems of 4096 particles with PBC's only away from criticality.

For $N=1024$, many of our runs went on for 10^8 MC sweeps, at least 2×10^8 MC sweeps were performed on 10 runs in the transition region. For $N=256$ and 64 runs need not be as long. We executed 10 runs in the $(5–15)\times 10^7$ MCS sweeps range. Many additional shorter runs were performed, away from the transition region, for each of these systems.

III. VOLUME FLUCTUATIONS

In this section, we report results for the mean volume $\langle v\rangle$, its fluctuations $\langle(\delta v)^2\rangle$, and for its probability distribu-

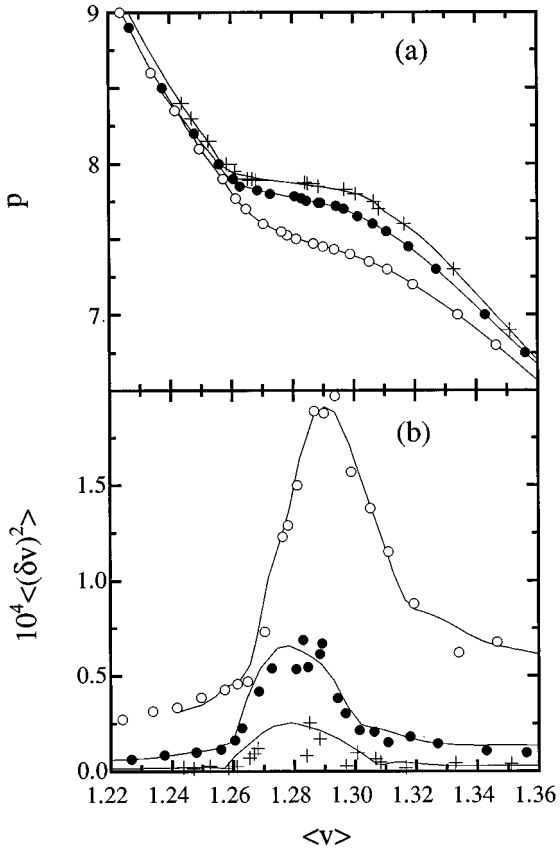

FIG. 5. (a) Data points for p vs volume for systems of (○) 900, (●) 3844, and (+) 15 876 disks, with HCW's. p is given in units of kT/a_0, and that a_o is the closest packing value of the specific volume, and v is in units of a_o. Error bars, which are horizontal, are of about the size of the data points shown. (b) $\langle(\delta v)^2\rangle$ vs $\langle v\rangle$ for the same systems as in (a). Full lines are for $-\partial v/\partial p$, obtained from cubic spline fits to $p(v)$ curves in (a). The points shown are obtained from fluctuations.

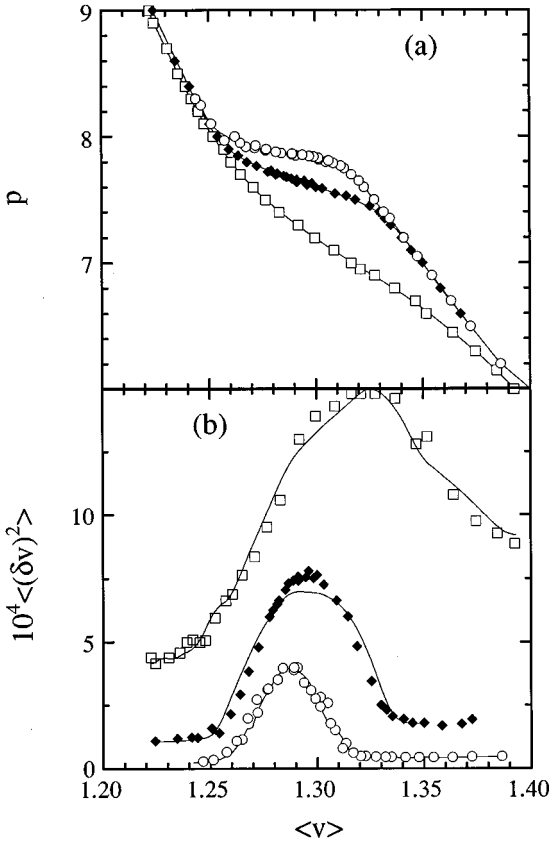

FIG. 6. (a) Data points for p vs v for systems of (□) 64, (◇) 256, and (○) 1024 disks, with PBC. p is given in units of kT/a_0, and that a_o is the closest packing value of the specific volume. Error bars, which are horizontal, are of about the size of the data points shown. (b) $\langle(\delta v)^2\rangle$ versus $\langle v\rangle$ for the same systems as in (a). Full lines are for $\partial v/\partial p$, obtained from cubic spline fits to $p(v)$ curves in (a). The points shown are obtained from fluctuations.

tion $P(v)$. The main body of evidence that supports our conclusion that melting in two dimensions is a second order transition is given in this section.

A. Volume fluctuations

Data points obtained for $\langle v\rangle$ as a function of p are plotted as p versus $\langle v\rangle$ in Figs. 5(a) and 6(a) for HCW's and PBC's, respectively. The continuous lines shown are cubic spline fits to the data. Data points for $\langle(\delta v)^2\rangle$ are shown in Figs. 5(b) and 6(b) for HCW's and PBC's, respectively. [The continuous lines shown follow, using the relation $\partial\langle v\rangle/\partial p=-N\langle(\delta v)^2\rangle$, from derivatives (taken numerically) of the cubic spline fits for $p(v)$.] The agreement between the data points (obtained from fluctuations throughout MC runs) and the continuous lines shown in Figs. 5(b) and 6(b) is a measure of the quality of our equilibrium results. We determine the melting point volume value, $v_m=1.259\pm0.006$, from the Bulk modulus data shown in Fig. 7.

We wish to establish whether there is a latent heat in order to diagnose the order of the transition. Since the energy of hard disks is zero, the latent heat (per particle) is given by $p\Delta v$. Δv can be determined from data for $\langle(\delta v)^2\rangle$; for macroscopic systems, $\langle(\delta v)^2\rangle$ is nonvanishing in the coexistence region of a first order phase transition. More quantitatively, a plot of $\langle(\delta v)^2\rangle$ versus $\langle v\rangle$ would give a parabola for a first order phase transition; its maximum value would be $(\Delta v)^2/4$, and it would vanish at $v=v_1$ and $v=v_2$ (v_1 and v_2 are the specific volumes of each of the two hypothetical phases). Inspection of Figs. 5(b) and 6(b) shows that the maximum value of $\langle\delta v^2\rangle$ is cut down by factors of about 3 and 2, respectively, whenever $N\to4N$. Furthermore, even if this trend were not sustained as $N\to\infty$, even a value as large as 5×10^{-5}, say, for the $N\to\infty$ limit value of the maximum of $\langle\delta v^2\rangle$ [see Fig. 5(b)], would still imply $\Delta v\simeq0.014$. Clearly, the volume discontinuity of a first order transition, if one were to exist, would have to be within a range of approximately $0.01v_m$. This value is several times smaller than the values often given by MC simulations that diagnose a first order transition [20,29], and half as large as the value given more recently in Ref. [22]. Our results are, however, in agreement with the trend suggested by Zollweg and Chester for the tie line [21]: that $\Delta v<0.025$ for a system of $N=16\,384$ with PBC's, and from exploratory runs for $N=65\,536$ particles they suggested that Δv might vanish completely as $N\to\infty$.

Results for the bulk modulus B (given by $-v\partial p/\partial v$) are shown in Figs. 7(a) and 7(b) for systems with HCW's and

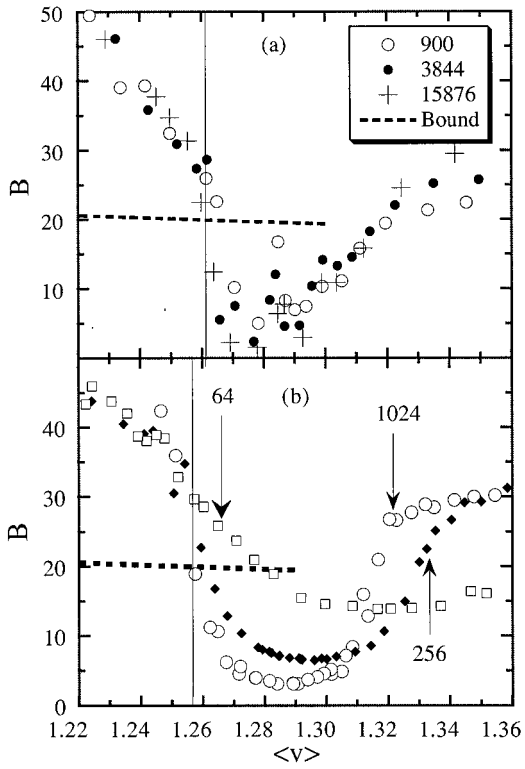

FIG. 7. (a) Bulk modulus vs volume for systems of various sizes (for the number of particles shown) with HCW boundary conditions. The data points follow from taking finite derivatives straightforwardly of the data points shown in Fig. 5(a). The vertical line is at the melting point value, $v_m = 1.261$. The dotted line is an upper bound that follows from the prediction of Nelson and Halperin involving the bulk and shear moduli at the melting point. See text for details. (b) Same as for (a) but for systems with PBC's. The data points shown here obtained from fluctuations, using $\partial\langle v\rangle/\partial p = -N\langle(\delta v)^2\rangle$.

PBC's, respectively. The data points in Fig. 7(a) follow from taking finite derivatives of the data shown in Fig. 5(a). This procedure gives data points with less scatter than would be obtained using values of $\langle(\delta v)^2\rangle$ through the relation $v/B = N\langle(\delta v)^2\rangle$. This relation and data for $\langle(\delta v)^2\rangle$ are used for plotting the points shown in Fig. 7(b) for systems with PBC's [for which our statistical errors are much smaller than for systems with HCW's, as Figs. 5(b) and 6(b) illustrate]. That B does not decrease as $1/N$ in any given volume range, as it would for a first order transition, is not as easily appreciated in Fig. 7 as it is in Figs. 5(b) and 6(b).

We can use the relation $1/\mu + 1/(\lambda+\mu) = v/4\pi$ (expressed in our own units for pressure and volume, where μ and λ are the Lamé constants of elasticity theory), derived for the melting point by Nelson and Halperin [4,5], to obtain a lower bound for B at the melting point. $B = \lambda + \mu$, which follows from a continuum elastic description of solids, is not expected to hold up to the melting point for systems of disks. Not having computed the value of μ, we obtain a bound for B replacing μ and $\lambda+\mu$ by the larger values $\lambda+\mu$ and B, respectively (see footnote 37 in Ref. [5]). The bound that follows, $B \geq 8\pi/v$, is shown as dotted lines in Figs. 7(a) and 7(b).

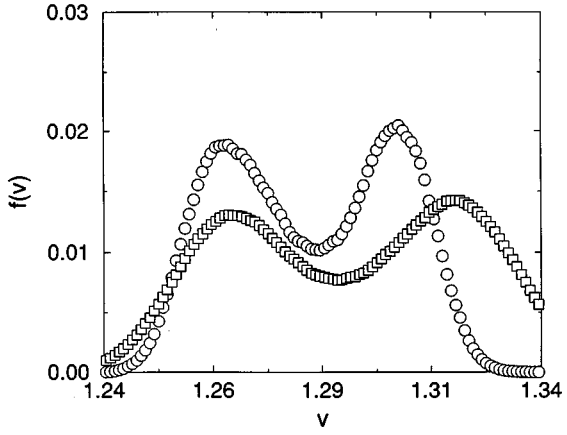

FIG. 8. Frequency of occurrence for the specific volume v for systems (with PBC's) of (□) $N = 256$ and (○) 1024 for $p = 7.865$ and $p = 7.65$, respectively. These data points follow from runs of over 2×10^8 MC sweeps. The data have not been smoothed.

B drops sharply near $v = 1.26$ in both Figs. 5(b) and 6(b). That behavior, in the vicinity of the melting point, is not surprising, since $-d(\lambda+\mu)/dv \to \infty$ at $v = v_m$ is predicted by the KTHNY theory [4]. A slight complication arises because $|dB/dv|$ itself remains finite in the KTHNY theory. This is because B has an *essential* singularity, given by $\partial^2 F/\partial v^2$ (as follows from the definition of B), and the singular part of the free energy, F, is ξ^{-2}, and $\xi \sim \exp[-b/(v-v_m)^{1/2}]$ in the KTHNY theory. Let the point where the maximum value of $|dB/dv|$ is located be v_m'. It does not follow rigorously that $v_m \leq v_m'$, but it seems quite unlikely that it be otherwise. We find $v_m' = 1.261 \pm 0.004$ and $v_m' = 1.257 \pm 0.005$ for HCW's and PBC's, respectively. Evidence for setting $v_m = v_m'$ is given in Sec. IV.

B. Volume distributions

We obtain the frequency of occurrence $f(v)$, for 0.001 wide Δv slots, from counting the number of times that the specific volume is found between values v and $v+\Delta v$ in a given MC run. Obviously, the probability density that a system's specific volume takes the value v fulfils $P(v) \propto f(v)$. $f(v)$ is shown in Fig. 8 for systems of 256 and 1024 particles with PBC's. Note how volume fluctuations decrease as N increases. This is in keeping with results of the previous subsection. Figures 9(a), 9(b), 9(c), and 9(d) illustrate how $f(v)$ varies with pressure in the range $7.80 \leq p \leq 7.90$, for $N = 1024$. The data points have not been smoothed. They were obtained from MC runs of over 2×10^8 MC sweeps. Much shorter runs give poor statistics.

More information about the nature of the melting transition follows from the knowledge of the free energy barrier ΔG that separates the high and low volume phases. ΔG must increase as the system's surface for a first order transition [23]. In order to obtain accurate values for ΔG, we first define an *assymmetry* variable q. Let f_2 and f_1 be the two maximum values of $f(v)$, and f_0 be its minimum value in between the two maxima. We define

$$q \equiv \frac{f_2 - f_1}{2 f_0}. \tag{1}$$

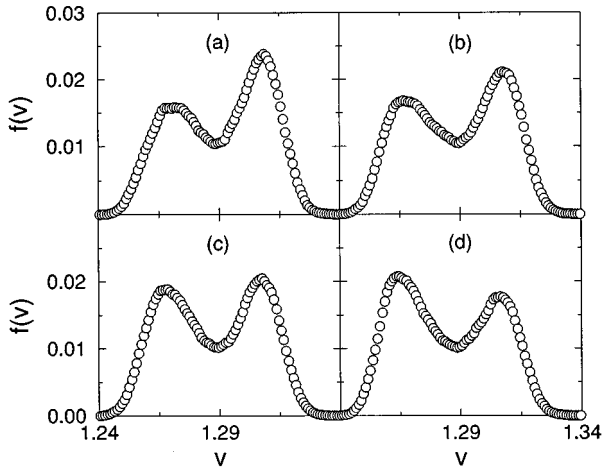

FIG. 9. (a) Frequency of occurrence for the specific volume v for a system (with PBC's) of $N=1024$ for $p=7.85$. These data points follow from runs of over 2×10^8 MC sweeps. (b) Same as in (a), but for $p=7.86$. (c) Same as in (a), but for $p=7.865$. (d) Same as in (a), but for $p=7.87$. The data have not been smoothed. All bins are for $\Delta v=10^{-3}$.

Whether it makes more sense to define q according to the areas under the two humps of $f(v)$ makes little difference here, because of the observed shape of $f(v)$. We define a free energy barrier $\Delta G(q)$ between the ''low'' and ''high'' volume phases,

$$e^{-\Delta G(q)/kT}=\frac{2f_0}{f_2+f_1}. \tag{2}$$

Data points for $\Delta G(q)/kT$ are shown versus $|q|$ in Fig. 10 for several system sizes ($N=256$, 576, and 1024). Data points obtained for $N=64$ and 400, from runs of over 10^8 MC sweeps are not shown in this figure.

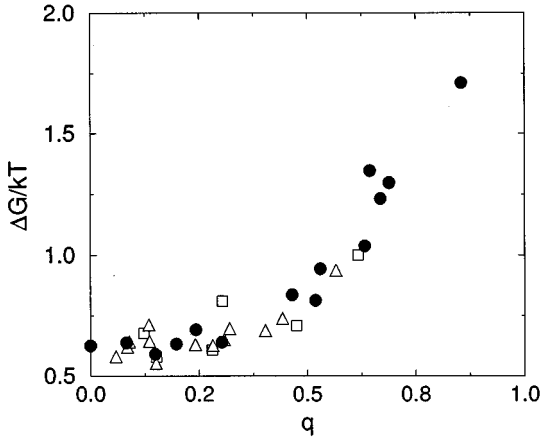

FIG. 10. Data points for $\Delta G/kT$ are plotted vs q, defined by $q\equiv|P_2-P_1|/2P_o$, where P_2 and P_1 are the two maximum values of $P(v)$, and P_o is its minimum value. △, □, and ● stand for $N=256$, 576, and 1024, respectively. Equation (2) is used to obtain the values of $\Delta G/kT$ shown. These points are obtained from data such as are shown in the previous figure for systems with PBC's.

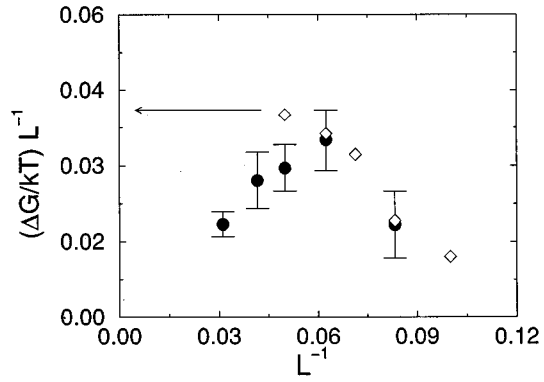

FIG. 11. Data points for $L^{-1}\Delta G/kT$ vs $1/L$. ◇ stand for data from Lee and Strandburg; ● are for our own data.

We let $\Delta G/kT$ be the $q\to0$ limit of $\Delta G(q)/kT$ (which we obtain with fourth order polynomial fits to the data). This procedure yields fairly accurate values for $\Delta G/kT$ (and its errors can be easily assessed). The values thus obtained for $L^{-1}\Delta G/kT$, as well as those obtained by Lee and Strandburg [20] for smaller systems, are displayed in Fig. 11 versus $1/L$. Clearly, the trend established for smaller systems by the data of Lee and Strandburg, that favors a first order transition, is reversed for larger systems.

We conclude this section with the following observation. $\Delta G/L$ can become independent of L only if the correlation length is smaller than the linear size of the system. Boundary conditions would not matter much then, and double humped graphs for $f(v)$ would therefore ensue for HCW also. Plots of $f(v)$ that contradict this assumption are shown in Fig. 12. Thus, it seems that, in the $N\to\infty$ limit, there is no volume

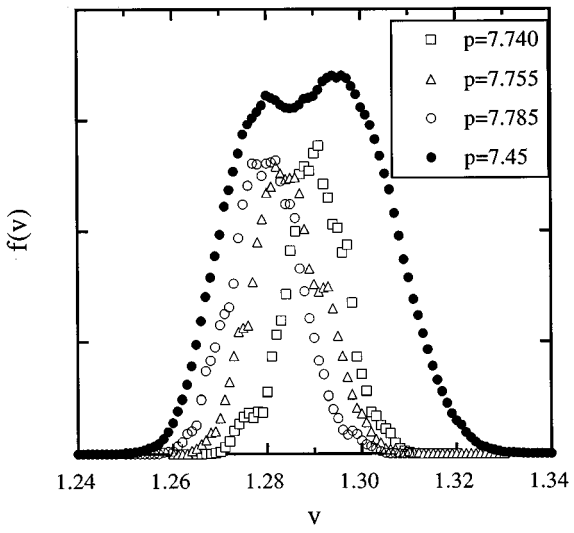

FIG. 12. Frequency of volume occurrences for systems with HCW boundary conditions. ● are for 900 particles. All other data points are for systems of 3844 particles, for the three pressure values shown. The data points for 900 particles are taken from a run of 10^8 MC sweeps. Other data points are taken from runs of (30–37) $\times10^7$ MC sweeps. Note that, for $N=3844$, $f(v)$ ''moves,'' as the pressure varies, in a fashion that is contrary to the existence of a double humped $f(v)$.

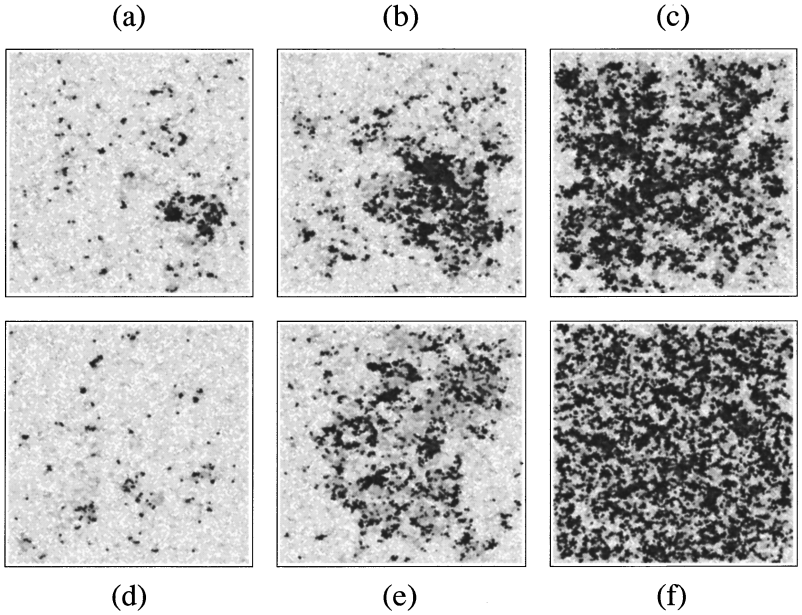

FIG. 13. Pictures show angle α as a function of position for each Voronoi cell, for systems with HCW's. White stands for $\alpha \simeq 0°$, and so on, up to black for $\alpha \simeq \pm 30°$. Picture (a) [(d)] is for the final state of the two runs shown in Fig. 1(a) that started from an ordered (disordered) state. Picture (b) [(e)] is for the final state of the runs shown in Fig. 1(b) that started from an ordered (disordered) state. The instantaneous volumes for (a), (d), (b), and (e) are 1.266, 1.265, 1.285, and 1.290, respectively. Two final states for $v \simeq 1.32$ and 1.35 are shown in (c) and (f), respectively.

discontinuity, and the free energy barrier between the two hypothetical phases becomes size independent.

IV. ORIENTATIONAL ORDER

We now turn our attention to the behavior of the orientational order parameter, more specifically of its average value, its fluctuations, and its probability distribution. We examine the evidence for the conclusion that the orientational order parameter vanishes discontinuously upon melting, and find that either there is no hexatic phase in 2D systems of hard disks, or else (if it exists) that the volume varies by less than about 1% in it.

A. Orientational order parameter

We define the orientational order parameter following Nelson and Halperin [4]. *Nearest neighbors* are defined first. Whether two particles are nearest neighbors may be decided by a rigorous scheme [30] that is a generalization of Wigner's cells for lattices, or through some *ad hoc* definition that makes use of particle distances only. We have used the former definition for the sort of crystalline maps that are shown in Figs. 13(a) and 15(a) (explained below), but have used the latter definition (for speed of execution) in our MC computer program. (In our computer program, two particles qualify as nearest neighbors if the square of the distance between them is less than 1.3 times the specific volume.)

We define the orientational order parameter in two steps. Let θ_n^m be the angle between the ''bond'' linking nearest neighbor particles n and m and some arbitrary reference line. An angle α_n (that shows how bonds out of particle n are oriented) is defined through the relation

$$a_n e^{i6\alpha_n} \equiv \frac{1}{z_n} \sum_m e^{6i\theta_n^m}, \tag{3}$$

where the sum is over all z_n nearest neighbors of the nth particle, and a_n is a real number that satisfies $0 \leqslant a_n \leqslant 1$. $a_n = 1$ for a perfectly crystalline configuration.

Spatial variations of α may be displayed in sort of maps, that we shall call bond orientation (BO) maps for short. Such maps are exhibited in Fig. 13 for the final configurations obtained from each of the four computer runs exhibited in Figs. 1(a) and 1(b), and for $v = 1.32$ and 1.35 for 15 876-particle systems. White stands for $\alpha \simeq 0°$, and increasingly darker grey scales are for other values of α, up to $\pm 30°$. The HCW boundary conditions force $\alpha \simeq 0$ near the walls. The two BO maps on the left hand side of the figure are for the two final configurations of Fig. 1(a), for which $p = 7.90$. The two BO maps on middle are for the final configurations of Fig. 1(b), for which $p = 7.875$. The top and bottom BO maps on the column at the right are for configurations with $v = 1.32$ and 1.35, respectively.

For comparison, we show graphs of the structure factor in Figs. 14(a) and 14(b)–14(f) for the final configurations whose BO maps are shown in Figs. 13(a) and 13(b)–13(f). Note the slight anisotropy shown by the graphs for $v \simeq 1.29$. This is to be expected, since the correlation length (see below) is nearly as long as the linear size of the system for $v = 1.29$.

No marked dependence on initial conditions is shown. Clearly, melting (loss of weak crystalline order) and loss of orientational order take place as v increases.

BO maps and crystalline structure graphs for systems with PBC's show similar behavior. Graphs and BO maps for $N = 1024$ and 4096 are displayed on the top and bottom row

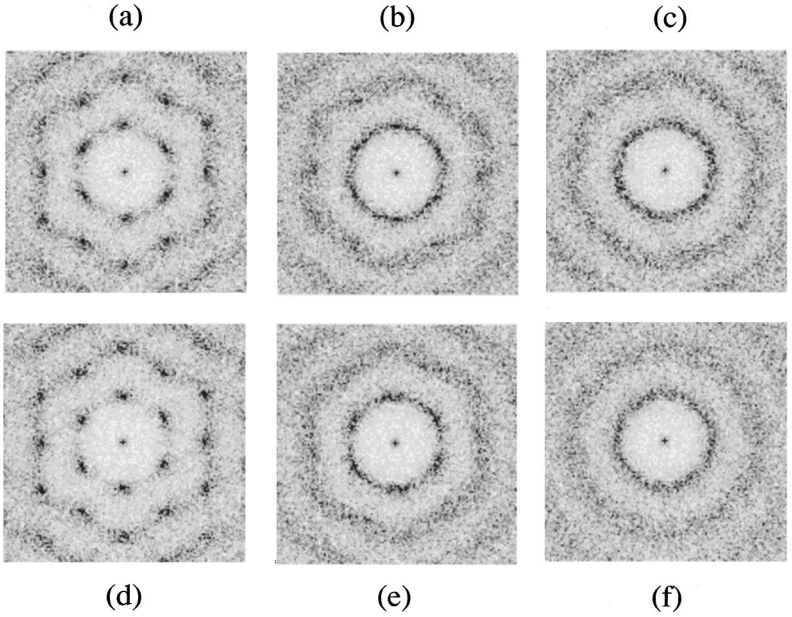

FIG. 14. Graphs show the structure factor $S(\mathbf{k})$ as a function of $\mathbf{k}=k_x,k_y$ for systems with HCW's. Graphs (a) and (b)–(f) are for the final configurations whose crystalline maps are shown in the previous figure.

of Fig. 15, respectively. Spatial variations of α are shown on columns 1 and 3. Each graph on columns 2 and 4 shows the structure factor for the configuration whose BO map is displayed on its left hand side. The left (right) half of the figure is for ordered (disordered) states with the same value of volume $v=1.26$ ($v=1.31$).

Note that orientational order is correlated on Fig. 15(c) over a distance that is comparable to the linear size of the $N=1024$ system. The maps of Fig. 15(g) are for a $N=4096$ system at a value of v (1.31) that is the same as for Fig. 15(c). Thus, whereas weak long-range orientational order might have been erroneously suspected from the BO map for the $N=1024$ system, the $N=4096$ system clearly exhibits many orientation domains. In fact, as will be seen below, $v=1.31$ is located deeply in the isotropic phase.

In order to be able to proceed with more quantitative considerations, we now conclude the definition of the orientational order parameter. Let

$$\phi_n \equiv a_n e^{i6\alpha_n}, \tag{4}$$

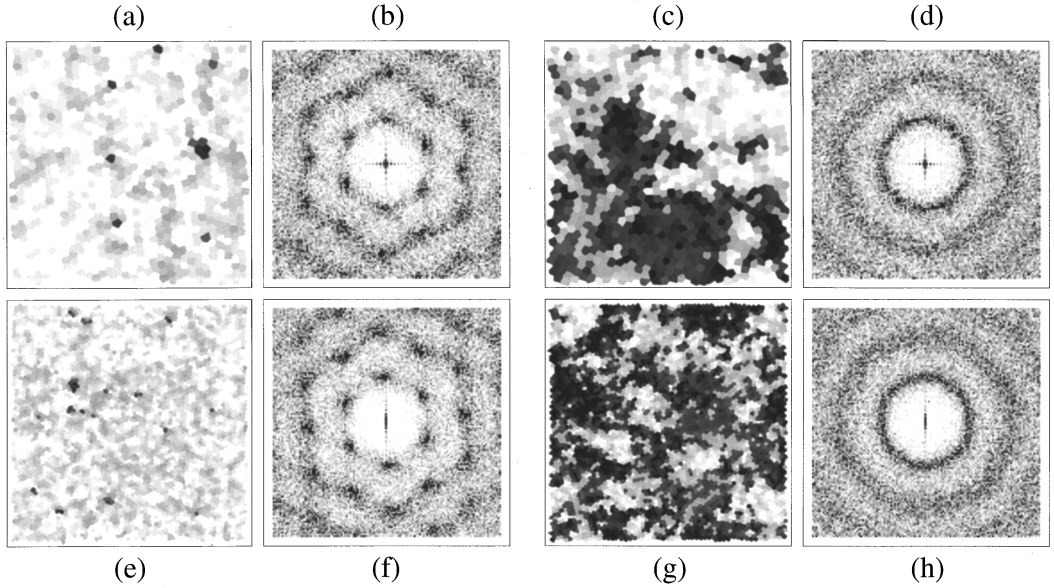

FIG. 15. Spatial variations of angle α [defined in Eq. (3)] are shown on columns 1 and 3, for systems with PBC's. Black stands for $\alpha=0°$, and so on, up to white for $\alpha=\pm 30°$. Structure factors $S(\mathbf{k})$ are shown as functions of k_1 (on the horizontal axis) and k_2 (on the vertical axis) on columns 2 and 4. The pair of pictures (a) and (b) [(e) and (f)] are for a configuration of $N=1024$ ($N=4096$) and volume $v=1.262$. The pair (c) and (d) [(g) and (h)] is for $N=1024$ ($N=4096$) and volume $v=1.318$. Graphs and BO maps for $N=1024$ and 4096 are displayed on the top and bottom rows, respectively.

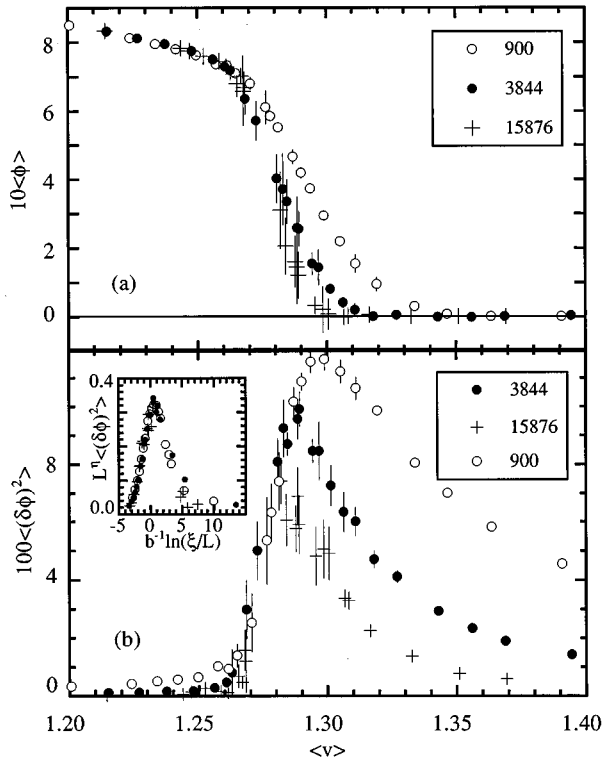

FIG. 16. (a) Quantity $\langle\phi\rangle$ vs $\langle v\rangle$ for the shown values of N hard disks in a box with HCW's. (b) $\langle|\delta\phi|^2\rangle$ vs $\langle v\rangle$ for various values [same as in Fig. 1(a)] of N hard disks; $\delta\phi\equiv\phi-\langle\phi\rangle$. $L^{\eta_6}\langle|\delta\phi|^2\rangle$ vs $b^{-1}\ln(\xi_6/L)$ is shown in the inset; $\eta_6=0.3$, $b=0.77$, $\xi_6=\exp(b/u^{1/2})$, $u=v-v_i$, and $v_i=1.260$.

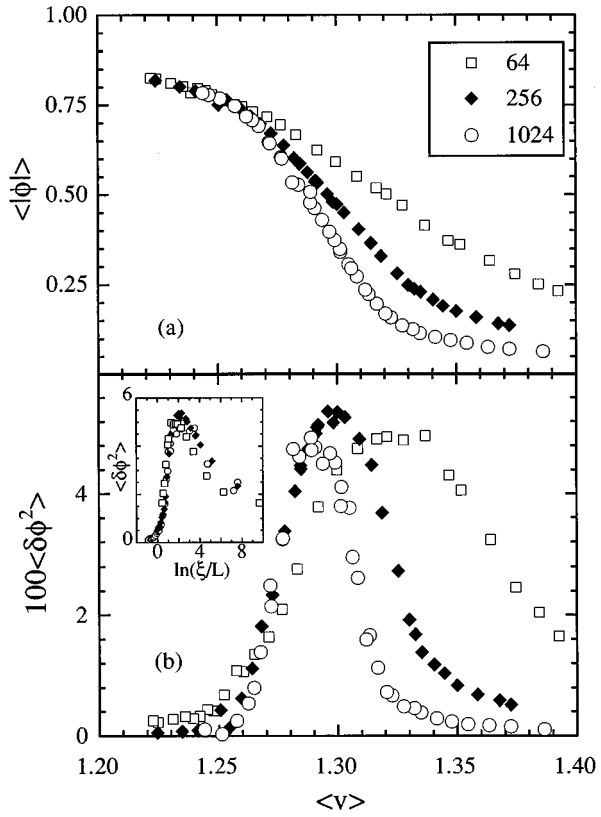

FIG. 17. (a) Quantity $\langle\phi\rangle$ vs $\langle v\rangle$ for systems with PBC and the number of particles shown. (b) $\langle|\delta\phi|^2\rangle$ vs $\langle v\rangle$ for the values of N shown in (a); $\langle|\delta\phi|^2\rangle$ vs $\ln(\xi_6/L)$ for the values of N shown in (a), $b=0.9$, $\xi_6=\exp(b/u^{1/2})$, $u=v-v_i$, and $v_i=1.265$. $\delta\phi\equiv\phi-\langle\phi\rangle$.

and

$$\phi\equiv\widetilde{N}^{-1}\sum_n \phi_n, \tag{5}$$

where the sum is over a set of $\widetilde{N}$ particles in the system. This is the definition of the orientational order parameter we use. For HCW boundary conditions, we only sum over particles within a small inner box (that holds $\widetilde{N}$ particles, and $\langle\widetilde{N}\rangle=N/16$) within the hard wall box. For PBC's the sum in the above equation is performed over all particles. ϕ gives a measure of order for systems that crystallize on triangular lattices. $\langle\phi\rangle=1$ for a perfectly crystalline triangular lattice, and $\langle\phi\rangle=0$ for a system in which the orientational symmetry is not broken. We do not take the absolute value of ϕ in the calculation of $\langle\phi\rangle$ for systems with HCW's. There is no need for it then because the HCW boundary conditions break the rotational symmetry of the system. For PBC's, average values of ϕ stand for $\langle|\phi|\rangle$. The reason for the absolute value is, of course, that $\langle\phi\rangle$ would otherwise vanish for all densities of any finite system with PBC's, since no spontaneous symmetry breaking can occur then.

Data points for $\langle\phi\rangle$ versus volume $\langle v\rangle$ are shown in Figs. 16(a) and 17(a) for systems of various sizes with HCW's and PBC's, respectively. We next argue that $\langle\phi\rangle$ vanishes discontinuously upon melting. The data for $\langle\phi\rangle$ show no size dependence for $\langle v\rangle<1.263$ for HCW's, nor for $\langle v\rangle<1.259$ for PBC's. Furthermore $\langle\phi\rangle\gtrsim0.75$ therein. Since we found in Sec. III that $v_m<1.261\pm0.004$ for HCW's, and that $v_m<1.257\pm0.005$ for PBC's, we conclude that $\langle\phi\rangle$ vanishes discontinuously at $v=v_m$, as predicted by Nelson and Halperin [4]. More specifically, $\langle\phi\rangle$ vanishes from the values 0.74 (at $v_m=1.261$) and 0.75 (at $v_m=1.257$), just below melting, for HCW's and PBC's, respectively. Independent evidence of this conclusion is to be found below in Sec. IV C. We take the mean of these two values ($v_m=1.259\pm0.006$) to be the melting volume value.

B. ϕ fluctuations

Definitions of the orientation correlation length ξ_6 and of the exponent η_6 follow from the general expression

$$\langle\phi_n\phi_l\rangle\sim e^{-r_{nl}/\xi}/r_{nl}^{\eta}, \tag{6}$$

where r_{nl} is the distance between particles n and l, and ϕ_n is defined in Eq. (4).

We now examine the behavior of $\langle|\delta\phi|^2\rangle$, where $\delta\phi\equiv\phi-\langle\phi\rangle$. Consider a plot of $\langle|\delta\phi|^2\rangle$ versus $\langle\phi\rangle$ for various system sizes. Since $\langle|\delta\phi|^2\rangle\sim1/N$ for $N^{1/2}\gg\xi_6$, it follows that $\langle|\delta\phi|^2\rangle\sim1/N$ for all nonzero values of $\langle\phi\rangle$, except for the critical region near $\langle\phi\rangle\approx0$ whose size vanishes as $N\to\infty$, if $\langle\phi\rangle$ vanishes *continuously* at the critical point. Such a behavior is illustrated in Fig. 18 for the Ising model in 2D, where fluctuations in magnetization are plotted versus the magnetization for systems of various sizes. That is

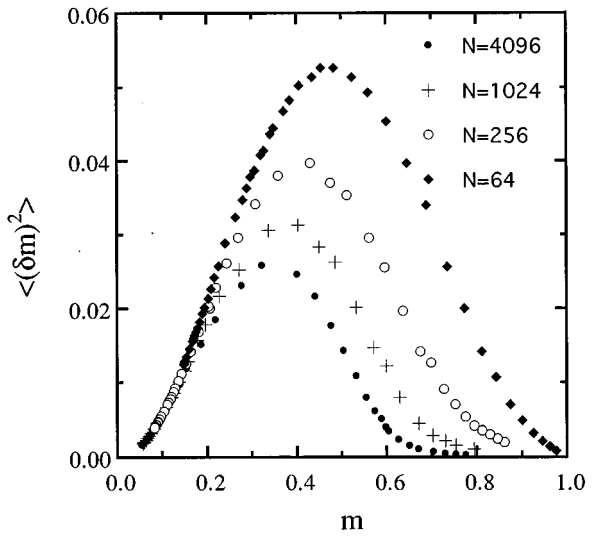

FIG. 18. Plots of magnetization fluctuations $\langle(\delta m)^2\rangle$ vs the magnetization m for two-dimensional Ising systems of $L=8$, 16, 32, and 64. As N increases, the range of values of m where $\langle(\delta m)^2\rangle$ does not decrease as $1/N$ becomes smaller, in accordance with m vanishing continuously at the critical point.

to be contrasted with the behavior exhibited in Fig. 19(a) and 19(b), for systems with HCW's and PBC's, respectively. The observed behavior is compatible with criticality over the entire interval $0\leqslant\langle\phi\rangle\lesssim 0.7$, that is, with a discontinuous drop from $\langle\phi\rangle\approx 0.7$ in the crystalline phase just below $v=v_m$ to $\langle\phi\rangle=0$ just above $v=v_m$. This is in agreement with the conclusion drawn in Sec. IV A.

We next examine how $\langle|\delta\phi|^2\rangle$ behaves as a function of volume in order to determine the extent of the isotropic phase. $\langle|\delta\phi|^2\rangle$ is expected to rise as $\langle v\rangle$ decreases, until the rise is arrested when the correlation length ξ_6 becomes as large as the linear size L of the system. Figures 16(b) and 17(b) show $\langle|\delta\phi|^2\rangle$ versus $\langle v\rangle$ for systems of various sizes, with HCW's and PBC's, respectively. Plots of $L^{\eta_6}\langle|\delta\phi|^2\rangle$ versus $b^{-1}\ln(\xi_6/L)$ data points collapse nicely into a seemingly universal curve, as shown in the inset of Fig. 16(b), after using $\xi_6=\exp(b/u^{1/2})$, where $u=|v-v_i|$, with $v_i=1.260$, $b=0.77$, and $\eta_6=0.3$, for systems with HCW's. This is in accordance with an isotropic phase that extends down to $v=v_i$, where ξ_6 (whose behavior we have prescribed using the KTHNY theory) diverges. Scattering of data points becomes significant for $|v_i-1.260|>0.005$. That, plus the corresponding variations of b and η_6, gives $v_i=1.260\pm 0.005$, $b=0.8\pm 0.1$, and $\eta_6=0.30\pm 0.05$.

The same procedure applied to the $\langle|\delta\phi|^2\rangle$ data for systems with PBC's, yields the results shown in the inset of Fig. 17(b) using $\xi_6=\exp(b/u^{1/2})$, and $v_i=1.265\pm 0.005$, and $b=0.9\pm 0.1$. Note that whereas $L^{\eta_6}\langle|\delta\phi|^2\rangle$ is scaled for HCW, the factor L^{η_6} is omitted for PBC's. This is because the best value of η_6 found for PBC's is $\eta_6=0$. The values found for v_i for PBC's and HCW's agree within statistical errors. So do the values found for b. However, the values found for η_6 clearly disagree. This is discussed in Sec. V.

Putting together results for HCW's and PBC's we arrive at $v_i=1.262\pm 0.007$. Since $v_m=1.259\pm 0.006$, we must conclude that v_i-v_m, the extent of hexatic phase (if there is one), lies unresolved within our statistical errors. More information about the hexatic phase is given in Sec. IV D.

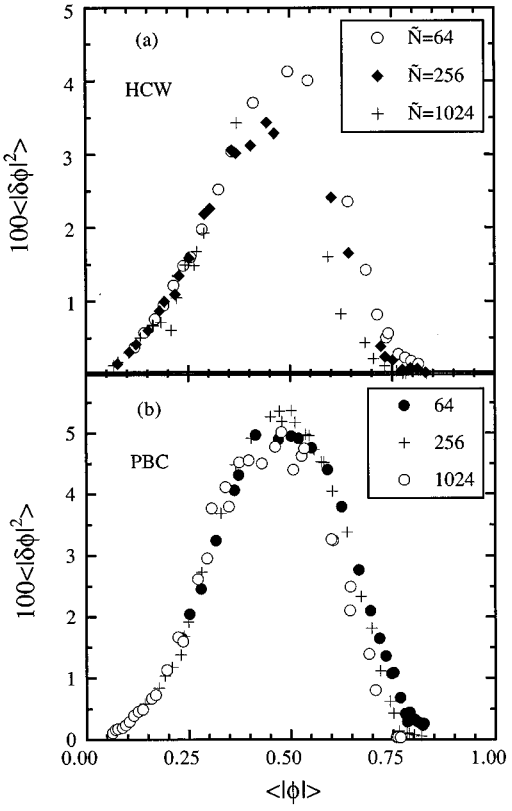

FIG. 19. (a) Data points for $\langle|\delta\phi|^2_{\sim}\rangle$ vs $\langle\phi\rangle$ for systems of various sizes, with HCW's. (Recall that $\tilde{N}$ is the number of particles in a subsystem that only holds 1/16 of the total number N of particles in the whole system.) (b) Same as in (a), but for systems with PBC's. The observed behavior is compatible with a critical behavior over the interval $0\leqslant\langle\phi\rangle\lesssim 0.7$; that is, with a discontinuity in $\langle\phi\rangle$ at the melting point.

C. ϕ distributions

This section is devoted to systems with PBC's. The corresponding results for systems with HCW's are uninteresting. (ϕ distributions for systems with HCW's behave much as volume distributions do: there are no double humps for any value of the pressure.) Let $P(|\phi|)$ be the (unrenormalized) probability density that the absolute value of the order parameter have a value within $|\phi|$ and $|\phi|+d|\phi|$. When ϕ is distributed isotropically, then $P(|\phi|)/|\phi|$ is proportional to the joint probability density for the real and imaginary parts of ϕ. For finite systems, $P(|\phi|)/|\phi|$ is centered on $\phi=0$ in the isotropic phase, well above the critical point, but it is centered on a nonzero value in the crystalline phase for $v\ll v_m$. It turns out that, for PBC's, $P(|\phi|)/|\phi|$ is ''doubled humped'' near the melting point. Such plots are shown in in Figs. 20(a)–20(d) for a system of 1024 particles under pressures $p=7.85$, 7.86, 7.865, and 7.87, respectively. Clearly, ϕ distributions are affected by pressure variations much as volume distributions are affected (see Fig. 9). Indeed, fluctuations in ϕ and v are correlated. This is discussed in Sec. V.

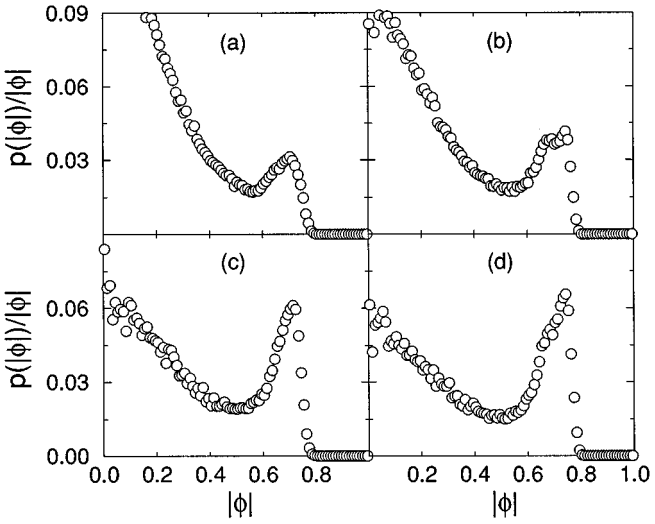

FIG. 20. Quantity $P(|\phi|)/|\phi|$ for systems of 1024 disks with PBC's. Figures (a), (b), (c), and (d) are for pressure values $p=7.85$, 7.86, 7.865, and 7.87, respectively. Data points for (a), (b), (c), and (d) are obtained from the same runs as data on Figs. 5(a), 5(b), 5(c), and 5(d). Each bin is for $\Delta|\phi|=10^{-3}$.

$P(|\phi|)/|\phi|$ versus ϕ is shown in Fig. 21 for $N=1024$, 576, and 256 for $p=7.87$, 7.83, and 7.66, respectively. The three distributions shown are remarkably alike. (A distribution of ϕ for $N=64$, that is not shown for the sake of clarity, differs negligibly from the rest.) Coexistence of two phases, one for $\phi=0$ and the other one for $\phi=0.74\pm0.02$, for macroscopic systems might (erroneously) be inferred from inspection of Fig. 21. Coexistence of two phases in a first order phase transition would imply a free energy barrier, between the $\langle\phi\rangle=0$ phase and the crystalline phase, that would increase as the surface of the system. However, no system size dependence is observed in Fig. 21. This fact is more obvious here than for volume fluctuations. The qualitative conclusion for the free energy barrier, however, is the same: it is size independent.

On the other hand, whereas the trend exhibited in Sec. III is consistent with *volume* fluctuations vanishing (for all pressures) in the $N\to\infty$ limit, $P(|\phi|)/|\phi|$ peaks at

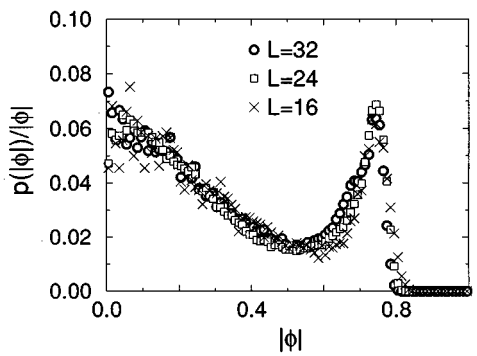

FIG. 21. Quantity $P(|\phi|)/|\phi|$ is shown vs $|\phi|$ for systems (with PBC's) of $N=256$ for $p=7.66$, $N=576$ for $p=7.83$, and $N=1024$ for $p=7.87$.

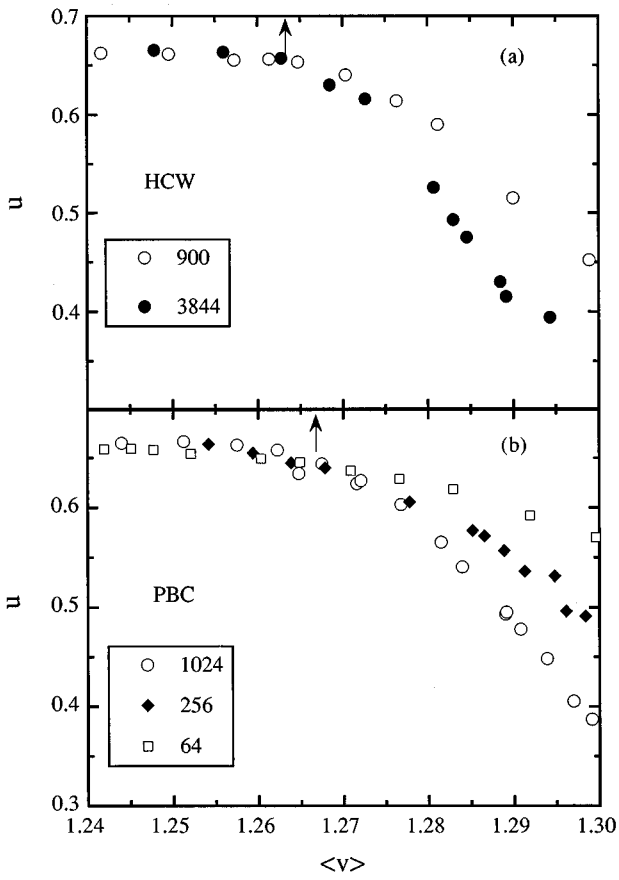

FIG. 22. (a) Data points for the fourth order cumulantlike quantity $u=1-\langle|\phi|^4\rangle/(3\langle|\phi|^2\rangle^2)$, vs volume, for systems with HCW's for the sizes shown. The arrow shows where curve fits to the data points for different system sizes meet. (b) Same as in (a), but for systems with PBC's for the sizes shown.

$\phi=0.74\pm0.02$, and no significant size dependence for it is observed. This contrasting behavior, between fluctuations in v and in ϕ, is discussed in Sec. V.

The peak location of $P(|\phi|)/|\phi|$ at $\phi=0.74\pm0.02$ provides an independent determination of the value of $\langle\phi\rangle$ just below melting. In addition, it follows from the data shown in Fig. 17(a) that the value $\langle\phi\rangle=0.74\pm0.02$ corresponds to $v=1.258\pm0.004$. This provides a check on the value of v_m established above by another method.

D. Cumulants

Fourth order cumulants have sometimes been used to locate critical points, and to diagnose whether a transition is of first or second order [31]. We report the results we obtained next. They are consistent with the conclusions arrived at thus far, but they lead us to nothing new.

Consider the fourth order cumulant $\Delta_4=\langle|\phi|^4\rangle-3\langle|\phi|^2\rangle^2$. In order to make comparison with other published work easier, we work with quantity u, given by $u=-\Delta_4/(3\langle|\phi|^2\rangle^2)$, which we will refer to as *the cumulant*. Clearly, $u=\frac{2}{3}$ for macroscopic systems in the crystalline phase, since $\langle\phi\rangle\neq0$ therein, and fluctuation contributions

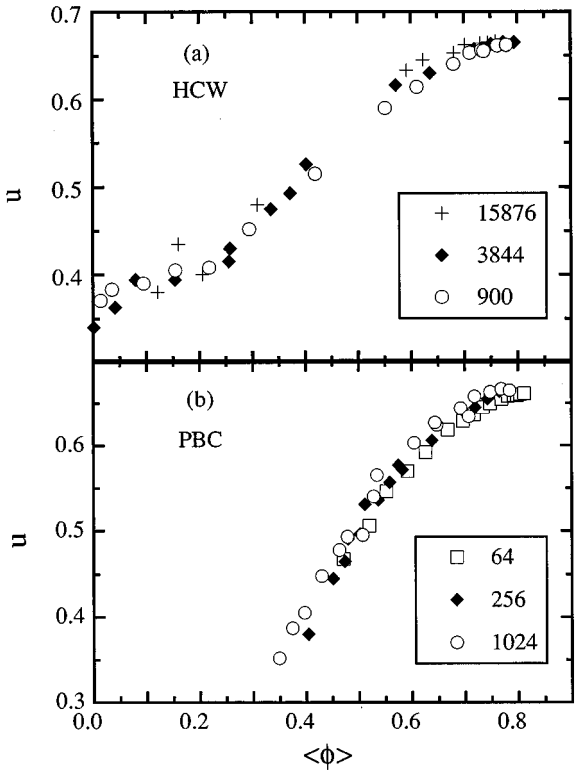

FIG. 23. Data points for the fourth order cumulantlike quantity $u=1-\langle|\phi|^4\rangle/(3\langle|\phi|^2\rangle^2)$, vs $\langle|\phi|\rangle$, for the system sizes shown. (b) Same as in (a), but for systems with PBC's for the sizes shown.

vanish for macroscopic systems. On the other hand, $u=\frac{1}{3}$ for macroscopic systems in the isotropic phase, since the central limit theorem then gives a *joint normal* probability density for the real and imaginary parts of ϕ. It is straightforward to show that u increases with system size (up to $\frac{2}{3}$) in the crystalline phase. u decreases with system size (down to $\frac{1}{3}$) in the isotropic phase. It has been argued (see Ref. [22] and references therein) that u would be size independent in the hexatic phase. Plots of u versus specific volume are shown in Figs. 22(a) and 22(b) for systems of 900 and 3844 particles (with HCW's), and for systems of 1024, 256 and 64 particles (with PBC's). Let v_c be the volume value such that cumulant curves are clearly size dependent for $v>v_c$, where u decreases as N increases. $v_c=v_i$ is expected. Polynomial (of second, third, and fourth order) fits to the data give $v_c=1.263\pm0.005$ for HCW's, and $v=1.267\pm0.005$ for PBC's. This is in agreement, within statistical errors, of the value ($v_i=1.262\pm0.007$) we have obtained for v_i.

It is instructive to plot u versus $\langle\phi\rangle$ for various system sizes, as shown in Figs. 23(a) and 23(b). The trend shown contradicts the hypothesis that $\langle\phi\rangle$ vanishes *continuously* upon melting, because if that were so, then $\langle\phi\rangle\neq0$ would imply a crystalline state, from which it would follow that u would increase with N (up to the value $\frac{2}{3}$ in the $N\to\infty$ limit) for any nonzero value of $\langle\phi\rangle$. Since u seems rather independent of N, and u is significantly smaller than $\frac{2}{3}$ for $\langle\phi\rangle\lesssim0.7$, a discontinuous drop in $\langle\phi\rangle$ upon melting follows once more.

V. CONCLUSIONS AND REMARKS

A. Conclusions

We first summarize our main conclusions. Specific volume fluctuations decrease as system size increases, in accordance with a second order phase transition [see Figs. 5(b) and 6(b)]. Further support for the melting transition in 2D being of second order follows from the observation (see Figs. 11 and 12) that the free energy barrier $\Delta G(v)$ for a fluctuation of volume v seems to become independent of system size for $N\gtrsim400$ at criticality. Thus the trend established previously [20] for $\Delta G(v)$ for $N\lesssim400$, that $\Delta G(v)$ grows as the system's surface area, is reversed for larger values of N. For hard crystalline walls, $\Delta G(v)\simeq0$, at least for $N\lesssim3844$ —see Fig. 12. Furthermore, $\Delta G(\phi)$ exhibits no size dependence throughout the full range of system sizes we studied with PBC's (see Fig. 21).

Our second conclusion is that $\langle\phi\rangle$ drops discontinuously (from $\langle\phi\rangle=0.74\pm0.02$) to zero at the melting point, as predicted by Nelson and Halperin. We draw this conclusion from three observations: (1) the size independence shown by $\langle\phi\rangle$ for $v\lesssim v_m$, the fact that $\langle\phi\rangle$ is far from vanishing therein, and the assumption that $\langle\phi\rangle=0$ for $v>v_m$; (2) the behavior of $P(|\phi|)/|\phi|$ at criticality (see Fig. 21); (3) the weak size dependence exhibited by $\langle|\delta\phi|^2\rangle$ for $0<\langle\phi\rangle\lesssim0.7$ [see Figs. 18, 19(a), and 19(b)]; and (4) the fourth order cumulant of ϕ as a function of $\langle\phi\rangle$ differs from the value ($\frac{2}{3}$) it must have in the crystalline phase, and seems to be size independent, for $0<\langle\phi\rangle\lesssim0.7$.

We find no hexatic phase. If it exists for systems of hard disks, then its extent is quite small and lies unresolved under our statistical errors. ($v_i-v_m=0.003$ is small with respect to the errors in v_i and v_m, which are 0.007 and 0.006, respectively.)

B. Remarks

Some caveats for the conclusions we have drawn from our *numerical* results follow. We cannot rule out a first order phase transition coexistence region, or a hexatic phase, in which the volume can vary by less than 1%. We cannot rule out either that $\langle\phi\rangle$ vanishes continuously at the critical point as, for instance, $\langle\phi\rangle\sim(v_m-v)^\beta$, for $v<v_m$, though consistency with our data would require that $\beta\lesssim0.1$. We estimate the latter bound as follows. Consider the plots shown in Figs. 18, 19(a), and 19(b). All data points for the Ising model with $N=64$, 256, and 1024 spins collapse into one seemingly universal curve if we plot $\langle(\delta m)^2\rangle L^{1/4+\epsilon}$ versus $\langle m\rangle L^{1/8+\epsilon/2}$; that is, if we shift the exponent values for the susceptibility and for m away from their correct value by ϵ and by $\epsilon/2$, respectively, where $\epsilon=0.14$. (Data points for $N=4096$ do not scale as well with the rest of the data, for these wrong exponent values.) Similarly, all our data points, for $\widetilde{N}=64$,256, and 1024 collapse surprisingly well into one curve when we plot $\langle|\delta\phi|^2\rangle L^\epsilon$ and $\langle\phi\rangle L^{\epsilon/2}$, where $\epsilon=0.15$. Unfortunately, we have no data available (as we do for the Ising model) that would allow us to check whether indeed scaling does become worse, with these exponents, for larger systems.

Our results for η_6 are inconclusive. For HCW's, $\eta_6 \simeq 0.3$ for $v > v_i$ follows from scaling $L^{\eta_6}\langle|\delta\phi|^2\rangle$ data for $v > v_i$ versus ξ_6/L. However, we obtain $\eta_6 = 0$ for PBC's. These two results are clearly contradictory. There are several ways out of this. One is that the hexatic phase does exist, but we cannot resolve it with systems of some 10^4 particles, and that we are picking up effects from the two critical points that would exist then. Such effects can be boundary dependent [influence from the melting critical point would account for the double peaked $P(|\phi|)/|\phi|$ curves that are shown in Fig. 21 for PBC's for volumes significantly larger than v_i, which in turn imply the result $\eta_6 = 0$ for PBC's] for small systems. The other possibility is that the hexatic phase does not exist for systems of hard disks, and that the nonzero value that we found for η_6 in the isotropic phase of systems with HCW's does not hold right down to the critical point. That would not be too surprising. We did not try to fit our data with a volume dependent η_6 (that might vanish rapidly as $v \to v_m$, much as it does for the superfluidity transition in two dimensions, where $\eta = 0$ for $T \geq T_0$, and $\eta \neq 0$ for $T < T_0$, but $\eta \to 0$ as $T \to T_0$ from below [32], where T and T_0 are the temperature and critical temperature, respectively). Some interpolation between $\eta_6 = 0$ at $v = v_m$ and $\eta_6 \simeq 0.3$ at, say, $v = 1.260 + 0.005$ would have little effect on our scaling plots. In any event, we cannot resolve this issue here.

Knowledge of $S(\mathbf{k})$ might be useful for diagnosing the existence of the hexatic phase. We do not report data for $S(\mathbf{k})$, except the graphs (for *instantaneous* configurations) shown in Fig. 14 for HCW's, and the graphs shown in Fig. 15 for PBC's. Our data for $S(\mathbf{k})$ do not add anything new to our conclusions about the hexatic phase. Bagchi, Andersen, Swope [25] recently obtained some data for $S(\mathbf{k})$ that support the existence of the hexatic phase, from MC simulations of large systems of particles that interact through $1/r^{12}$ pair potentials. The extent of the hexatic phase they found is quite small: in it, the density can only vary by about 1%. As stated above, the accuracy of our results does not allow us to resolve something as small as that. There may be a fundamental reason for this, as follows from the following simple argument. A reasonably well defined number of dislocations must be present in the hexatic phase lest its own character be blurred. But consider the effect of adding just one single dislocation to a system of, say, 10^4 hard disks. It would lead to distances between rows (100 of them) decreasing by 1%, which is at least twice as large as the effect produced by sweeping through the entire hexatic phase. It would follow then that $N \geq (2v/\Delta v)^2$ would have to be fulfilled (Δv is how much the volume can vary in the hexatic phase) in order for the hexatic phase to be clearly discernible. The systems we have studied here (of $N \leq 15\,876$) do not quite fulfil this criterion. On the other hand, Bagchi, Andersen, and Swope simulated systems of up to 65 536 particles (with softer pair potential interactions). That may explain why they can discern a small hexatic phase that we cannot.

We next relate our results to recent work that support a first order phase transition. We have already mentioned in this section how our results fit with the ones obtained by Lee and Strandburg for small systems from long MC runs [20]: the trend shown by their data, as system sizes increase, that led them to conclude that melting is a first order phase transition in 2D, is reversed for the larger systems we have studied. In addition, no free energy barrier (for the nucleation of another hypothetical phase) shows up in the data for systems with HCW boundary conditions. On the other hand, Weber and co-workers [22] concluded that melting is a first order phase transition in 2D, mainly from MC simulations (of about 2×10^6 MC sweeps) of systems of 16 384 hard disks. They draw their conclusions from data that differ from ours. Their cumulant curves for subsystems of up to 256 particles cross at $v = 1.2851 \pm 0.0007$. But this point lies in the isotropic phase (according to other analysis of their data). This contradiction is avoided if a first order phase transition ensues at some volume larger than $v = 1.2851$, thus preempting the approach to the critical point further on. This led Weber and co-workers [22] to diagnose a first order transition. Our own cumulant curves for different system sizes spread out (see Fig. 22) for $v > 1.263 \pm 0.005$ and $v > 1.267 \pm 0.005$, for HCW's and PBC's, respectively. Our cumulant results, clearly different from those of Ref. [22], fit well with all of our conclusions. (The small size of the systems whose cumulant values were reported in Ref. [22] may account for the difference between the results quoted therein and our own.)

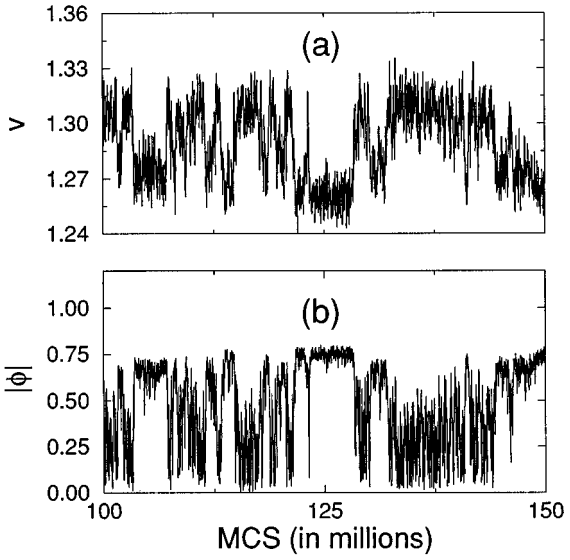

FIG. 24. (a) Time evolution of the volume v of a system (with PBC's) of 1024 disks for $P = 7.86$. (b) Time evolution of $|\phi|$, from the same portion of the run that data points in (a) are taken from. The ''time'' is in MC sweeps (given in millions).

Finally, we discuss the relation between the discontinuity in ϕ at $v = v_m$ and the lack of a corresponding discontinuity for v. Fluctuations in both of them are large at criticality, but $\langle(\delta v)^2\rangle$ vanishes as $N \to \infty$ [see Figs. 5(b), 6(b), and 8], which implies that there is no volume discontinuity. On the other hand, $\langle|\delta\phi|^2\rangle$ does not vanish as $N \to \infty$ [see Figs. 17(b) and 21], in accordance with a discontinuity in $\langle\phi\rangle$. This different behavior might seem somewhat puzzling, since v and ϕ fluctuations are strongly correlated. Figure 24 illustrates the point; time evolutions of $|\phi|$ and of v, taken from the same portion of a computer run, are shown for a system with $N = 1024$. Clearly, the system is coherently oriented at times when the volume is small, and becomes dis-

ordered when the volume is larger. In order to understand how finite fluctuations in ϕ may survive the $N \to \infty$ limit while finite fluctuations in v do not, consider a system with two domainlike regions, each with a given bond orientation. The volume is larger then only because there is a ''domain wall.'' (We use the word *domain* loosely here. Similar considerations would apply for disclinations.) Volume increments accompanying orientational disorder are domain *surface* effects. Not surprisingly, volume increments can be vanishingly small for fluctuations that take ϕ from a large value (e.g., 0.74) to a null value at criticality, in macroscopic systems. The results reported here were obtained from runs on a number of work stations that fluctuated, in about two years time, between about 5 and 15.

ACKNOWLEDGMENTS

We are indebted to Dr. Juan Rivero for greatly easing our interaction with computers. We are grateful to Dr. Juan Murgich and to Dr. Felix Carrique for generous help with computer work. We thank Professor E. Brézin, Professor M. Mezard, Professor H. Herrmann, and Professor D. Nelson for helpful comments. One of us (J.F.F.) is grateful for financial support from Junta de Andalucia, and another one of us (J.J.A.) is grateful for a study grant from Dirección General de Ciencia y Tecnología.

[1] R. E. Peierls, Helv. Phys. Acta Suppl. **7**, 81 (1936).
[2] L. D. Landau, Phys. Z. Sowjetunion **11**, 26 (1937); *Collected Papers of Landau* (Pergamon, London, 1967), p. 193.
[3] N. D. Mermin, Phys. Rev. **176**, 250 (1968).
[4] D. R. Nelson, Phys. Rev. B **18**, 2318 (1978); B. I. Halperin and D. R. Nelson, Phys. Rev. Lett. **41**, 121 (1978); D. R. Nelson and B. I. Halperin, Phys. Rev. B **21**, 5312 (1980); see also D. R. Nelson, *ibid.* **26**, 269 (1982); A. P. Young, *ibid.* **19**, 1855 (1979); For an alternate theory of 2D melting, see S. T. Chui, Phys. Rev. Lett. **48**, 933 (1982); Phys. Rev. B **28**, 178 (1983).
[5] D. R. Nelson and B. I. Halperin, Phys. Rev. B **19**, 2457 (1979).
[6] J. M. Kosterlitz and D. J. Thouless, J. Phys.C **6**, 1181 (1973); J. M. Kosterlitz, *ibid.* **7**, 1046 (1974).
[7] D. S. Fisher, B. I. Halperin, and R. Morf, Phys. Rev. B **20**, 4692 (1979); S. T. Chui, *ibid.* **28**, 178 (1983).
[8] For reviews and further references of older work, see D. W. Oxtoby, Nature **347**, 725 (1990); R. J. Birgeneau and P. M Horn, Science **232**, 329 (1986).
[9] C. A. Murray and D. H. Van Winkle, Phys. Rev. Lett. **58**, 1200 (1987).
[10] For recent experimental work and references therein, see R. Seshadri and R. M. Westervelt, Phys. Rev. Lett. **66**, 2774 (1991); Phys. Rev. B **46**, 5142 (1992); Phys. Rev. Lett. **70**, 234 (1993); R. E. Kusner, J. E. Mann, and A. J. Dahm, Phys. Rev. B **51**, 5746 (1995).
[11] N. A. Metropolis, A. W. Rosenbluth, M. N. Rosenbluth, A. H. Teller, and E. Teller, J. Chem. Phys. **21**, 1087 (1953); B. J. Alder and T. E. Wainwright, Phys. Rev. **127**, 359 (1962); L. Verlet and D. Levesque, Physica **36**, 254 (1967).
[12] W. W. Wood, in *Physics of Simple Liquids*, edited by H. N. V. Temperley, J. S. Rowlinson, and G. S. Rushbrooke (Wiley, New York, 1968), pp. 114–230; I. R. McDonald, Mol. Phys. **23**, 41 (1972).
[13] D. Frenkel and J. P. McTague, Phys. Rev. Lett. **42**, 1632 (1979).
[14] S. Toxvaerd, Phys. Rev. A **24**, 2735 (1981); Phys. Rev. Lett. **51** 1971 (1983); **53**, 2352 (1984).
[15] C. Udink and J. van der Elsken, Phys. Rev. B **35**, 279 (1987).
[16] A. F. Bakker, C. Bruin, and H. J. Hillhorst, Phys. Rev. Lett. **52**, 449 (1984).
[17] For reviews of Monte Carlo work, see K. J. Strandburg, Rev. Mod. Phys. **60**, 160 (1988); and in *Bond Orientational Order in Condensed Matter Systems*, edited by K. J. Strandburg (Springer, New York, 1992); M. A. Glaser and N. A. Clark, Adv. Chem. Phys. **83**, 543 (1993). For a recent account of a molecular dynamics simulation, and references therein, see W. Vermöhlen and N. Ito, Int. J. Mol. Phys. C **5**, 1021 (1994).
[18] F. F. Abraham, Phys. Rev. Lett. **44**, 463 (1980); J. A. Barker, D. Henderson, and F. F. Abraham, Physica A **106**, 226 (1981).
[19] K. J. Strandburg, J. A. Zollweg, and G. V. Chester, Phys. Rev. B **30**, 2755 (1984).
[20] J. Lee and K. J. Strandburg, Phys. Rev. B **46**, 11 190 (1992).
[21] J. A. Zollweg and G. V. Chester, Phys. Rev. B **46**, 11 186 (1992).
[22] H. Weber and D. Marx, Europhys. Lett. **27**, 593 (1994); H. Weber, D. Marx, and K. Binder, Phys. Rev. B **51**, 14 636 (1995).
[23] J. Lee and J. M. Kosterlitz, Phys. Rev. B **43**, 1268 (1991); E. Granato, J. M. Kosterlitz, J. Lee, and M. P. Nightingale, Phys. Rev. Lett. **66**, 1090 (1991).
[24] J. F. Fernández, J. J. Alonso, and J. Stankiewicz, Phys. Rev. Lett. **75**, 3477 (1995).
[25] K. Bagchi, H. C. Andersen, and W. Swope, Phys. Rev. Lett. **76**, 255 (1996).
[26] For a different perspective on a hexatic phase, see the recent publications, P. Blandon and D. Frenkel, Phys. Rev. Lett. **74**, 2519 (1995); T. Chow and D. R. Nelson (unpublished).
[27] It has been also been suggested before in J. Tobochnik and G. V. Chester, Phys. Rev. B **25**, 6778 (1982); J. A. Zollweg, G. V. Chester, and P. W. Leung, *ibid.* **39**, 9518 (1989).
[28] N. N. Bogolyubov, Physica **26**, S1 (1960).
[29] K. J. Strandburg, Rev. Mod. Phys. **60**, 160 (1988).
[30] Voronoi cells are defined in M. Senechal, Science **260**, 1170 (1993); A. Gervais, J. P. Troadec, and J. Lemaitre, J. Phys. A **25**, 6169 (1992).
[31] M. S. S. Challa and D. P. Landau, Phys. Rev. B **33**, 437 (1986).
[32] N. Schultka and E. Manousakis, Phys. Rev. B **49**, 12 071 (1994).